Research Article | Vol. 32, No. 20 / 23 Sep 2024 / Optics Express 35542
Optics EXPRESS

Impact of the Ge-Si interfacial barrier on the temperature-dependent performance of PureGaB Ge-on-Si p$^+$n photodiodes

LOVRO MARKOVIĆ,[1,*] TIHOMIR KNEŽEVIĆ,[2] LIS K. NANVER,[3] ASMA ATTARIABAD,[3] KHALIFA M. AZIZUR-RAHMAN,[4] JASMINE J. MAH,[4] KANG L. WANG,[5] AND TOMISLAV SULIGOJ[1]

[1]*Faculty of Electrical Engineering and Computing, University of Zagreb, Zagreb, Croatia*
[2]*Ruđer Bošković Institute, Zagreb, Croatia*
[3]*Faculty of Electrical Engineering, Mathematics & Computer Science, University of Twente, Enschede, Netherlands*
[4]*Center for Integrated Nanotechnologies, Sandia National Laboratories, Albuquerque, New Mexico, USA*
[5]*Department of Electrical and Computer Engineering, University of California, Los Angeles, California, USA*
[*]*lovro.markovic2@fer.hr*

Abstract: A temperature-dependent study of the near-infrared (NIR) responsivity of Ge-on-Si photodiodes is presented. The diodes, formed as n-Ge islands within oxide windows on n-Si and capped with Ga and B layers (PureGaB), exhibit low dark current of $\sim 2 \times 10^{-13}$ A/μm^2 and broadband responsivity. Temperature-dependent measurements reveal an inherent potential barrier at the low-doped n-Ge on the n-Si heterointerface. This leads to a decrease in responsivity with decreasing temperatures for wavelengths above 1100 nm. The Al-migration process along the Ge-Si interface, associated with the sidewall passivation and found to be a means of reducing dark current, increases the barrier height. Irrespective of the barrier height, room-temperature responsivity is fully recovered by applying a reverse bias to lower the interface barrier. In the devices with the highest barrier, the responsivity at 1310 nm increased from 4.8 to 164 mA/W, at 0 V and 18 V reverse bias, respectively. An additional increase in maximum responsivity at 1550 nm is attributed to Al-sidewall passivation leading to a measured responsivity of 126.4 mA/W at 18 V reverse bias.

© 2024 Optica Publishing Group under the terms of the Optica Open Access Publishing Agreement

1. Introduction

Germanium photodetectors are widely used for their near-infrared (NIR) light detection due to high absorption at the standard telecom wavelengths of 1310 and 1550 nm, superior carrier mobility compared to silicon, and lower fabrication cost compared to III-V NIR detectors [1,2]. On-chip fabrication of Ge devices, together with Si CMOS technology, enhances integration with support circuitry, improving device performance and reducing fabrication costs [2]. The push towards Si-based photonic integrated circuits (PICs) has also motivated the development of monolithically integrated Ge photodiodes with low dark currents and high responsivity. This technology is up-and-coming for various applications such as scattered light detection in ultra-low power detector scenarios [3], single photon detection [4], free space communication [5], and next-generation automotive LIDAR (Light Detection and Ranging) where photons are received at 1550 nm [6]. Additionally, Ge-on-Si photonics plays a crucial role in on-chip communication, as Ge serves as both a NIR detector and a low-loss waveguide material, extending its utility up to mid-IR wavelengths on SOI substrates [7]. However, Ge-on-Si integration can be difficult due to its potentially high threading dislocation density (TDD) making the fabrication of leakage-free and optically highly sensitive devices particularly challenging [8].

#530466 https://doi.org/10.1364/OE.530466
Journal © 2024 Received 25 Jun 2024; revised 30 Jul 2024; accepted 7 Aug 2024; published 18 Sep 2024

Optics EXPRESS

This paper presents an extended study of PureGaB Ge-on-Si photodiodes. A CMOS-compatible chemical-vapor deposition (CVD) technique was used to deposit Ge islands in oxide windows to the Si with a low TDD $< 10^7$ cm^{-2} [9]. This was followed by in-situ deposition of B and Ga layers (PureGaB) to create an anode region with a shallow, graded, p-type doping profile without surface roll-off [10,11]. When deposited on n-type Ge, PureGaB forms an asymmetric p-n junction with a highly-doped p-side, acting as an efficient barrier for electron injection. With this damage-free anode fabrication, it was possible to fabricate photodiodes with very low dark current density, $< 2 \times 10^{-13}$ A/μm^2 at 300 K, and 1 V reverse bias [12]. As a result, similar PureGaB photodiodes demonstrated a dark count rate below 1 kHz at room temperature (RT) in Geiger mode operation [13]. In [14,15] they were also shown to have broadband responsivity as verified for monochromatic wavelengths from 255 nm to 1550 nm.

Previously, it was demonstrated that the dark current was lowered when the Ge island sidewalls became passivated by an Al-mediated material transport of Ge and Si [16,17]. This transport took place during the alloying of the Al contact metallization around the perimeter of the Ge islands. On the Ge surface, the Ge was protected from interaction with Al by the B-layer which serves as a material barrier to many metals [18]. However, the material transport process also continued from the sidewalls to the Ge-Si interface. This was found to result in some reduction of the responsivity as it could introduce p-type doping. It was also concluded by TCAD simulations that only the acceptor states on the Ge-Si interface impact the responsivity of the device, while donor states did not [14]. Even though acceptor states could inherently exist at the Ge-Si interface [19], prolonging the Al alloying during device fabrication resulted in a further reduction of RT responsivity in the ultraviolet to NIR range [14]. This effect is further examined in this paper through measurements performed at temperatures from 300 K, 250 K, 150 K, and 77 K, that add to the understanding of the underlying physical mechanisms.

2. Fabrication and experimental setup

The fabrication of the PureGaB Ge-on-Si diodes was described in detail in [9]. We focus on an additional characterization of the devices fabricated in 26×26 μm^2 windows to the Si, a cross-section of which is shown in Fig. 1(a). The Ge islands and the PureGaB anodes were grown consecutively, without vacuum break, in an ASM Epsilon 2000 CVD reactor. While the Ge was grown using well-proven methods for achieving low defect densities, the p-type region was formed using a lesser-known method by first depositing a wetting layer of pure Ga at 400°C, and then a few nanometers of pure B at 700°C, in this case 11 nm. This method is a straightforward way to achieve damage-free anode fabrication, and it has recently also been shown that a p$^+$n-like junction can also be formed by depositing solely B under appropriate conditions [20]. Such devices can be contacted directly by Al, as the B layer acts as a robust material barrier between Al and Ge [16,18].

The Ge-islands were covered with 1-μm-thick plasma-enhanced CVD oxide. Then 1-μm-wide contact windows along the perimeter of the Ge islands were formed by lithography and plasma-etching. This step further resulted in a ∼100 nm gap in the B-layer (Fig. 1(a)), exposing the Ge perimeter to the subsequently sputtered Al metallization layer. The device was annealed at 400°C for 30 min which will be subsequently referred to as the alloying step. This alloying step facilitated the Al-mediated displacement of Ge and Si. As seen in the high-resolution transmission electron microscopy (HRTEM) image in Fig. 1(b), a large displacement of Al, Ge, and Si is visible in about the first 5 μm of the Ge-island perimeter. In the rest of the diode, no visible displacements were identified. Due to the Al contacting of the whole diode perimeter, the area of the light entrance window is 576 μm^2 (24×24 μm^2). The Al is known to p-dope both Ge and Si during migration [21,22]. Therefore, the area with significant displacement of Ge and Si is expected to be converted to a p-region, which would reduce the light-sensitive area of the diodes. For comparison, an additional set of diodes was characterized, where the same

Optics EXPRESS

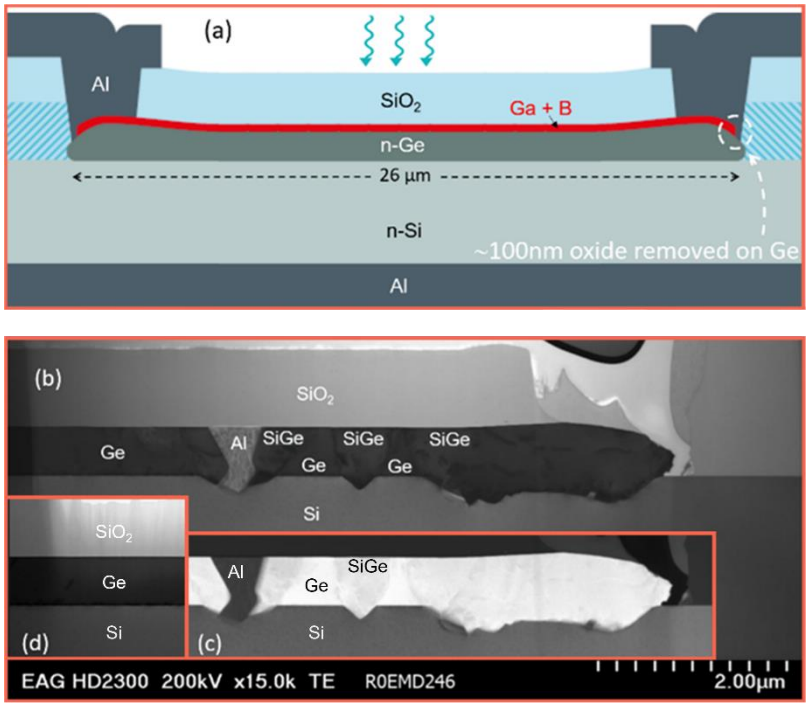

Fig. 1. (a) Schematic cross-section of a PureGaB Ge-on-Si diode. (b), (c) HRTEM images of the perimeter of a fabricated PureGaB diode indicating the material transport of Al, Ge and Si. In inset (d) an image of the central diode region is shown. The Ge thickness was determined from the HRTEM images, using the length bar at the bottom right.

fabrication process was followed, but a longer Al-alloying step of 60 minutes was applied, thus enhancing the material migration process.

The diodes were bonded to a 68-pin LCC case and mounted in a Janis ST-500 flow cryostat, allowing temperature control down to 77 K. Electrical measurements were performed using a HP 4156C parameter analyzer. Optical characterization was performed by Fourier-transform infrared spectroscopy (FTIR) using 0 V to 5 V reverse bias, as limited by the equipment. A broadband white light source was focused on the device under test (DUT) using an optical microscope coupled to the ThermoFisher Nicolet iS20 FTIR spectrometer, equipped with a deuterated L-alanine doped triglycine sulfate (DLaTGS) reference detector. A low-noise current preamplifier (SR570) amplified the photocurrent from the DUT and fed it to the spectrometer. The spectrometer software performed interferometer-based deconvolution to obtain a photocurrent spectrum of the device. The FTIR resolution varied from about 0.02 nm at 900 nm to 0.06 nm at 1550 nm incident wavelength. A correction procedure was performed using the reference DLaTGS detector to account for the instrument transfer function and spectral variations in the intensity of the incident light [23]. The corrected spectrum was calibrated for absolute response using two monochromatic responsivity measurements on the same devices at 2 V reverse bias. They were repeated three times, yielding average responsivity values of 58 mA/W and 34 mA/W at 1310 and 1550 nm, respectively [14].

Additional monochromatic measurements were performed at RT using the parameter analyzer, up to 18 V reverse bias. A Thorlabs MCLS1 laser source was used at 1310 nm and 1550 nm. It was fiber coupled to a microscope, used to focus the beam to the center of the device. The incident beam diameter is estimated to be below 20 µm. This generated photocurrents within

Optics EXPRESS

the linear operating area of the detector. The incident optical power was determined using a commercial Ge reference photodetector. The incident optical power on the DUT was constant within one experiment but varied from device to device between 2 to 13 μW due to the need to re-position and refocus the beam. This did not directly influence the responsivity since the photodiodes had linear power/photocurrent response in that power range, but varying reflections from the surrounding metal tracks and small power fluctuations resulted in a notable spread in responsivity as presented in Section 3. Measurements were repeated on 18 different diodes, 9 with 30-min and 9 with prolonged 60-min Al-alloying times.

3. Results and discussion

The spectral responsivity of a PureGaB photodiode was first acquired at RT and a reverse bias of 0 V, 2 V, and 5 V, as shown in Fig. 2(a). The maximum IR responsivity below the Si bandgap absorption edge at 300 K was 70 mA/W at 1365 nm and 5 V reverse bias. The exact spectral shape depends on reflectance from the surface and internally within the device layers. However, from the infrared peak, responsivity is reduced towards longer wavelengths due to a decrease in IR absorption. This is mainly due to absorption depths exceeding the 500 nm thickness of Ge for all wavelengths above 1100 nm [24]. The absorption length increases with increasing wavelength, thus the optical response is expected to decrease at longer wavelengths. The maximum achievable responsivity at longer wavelengths could be improved by increasing the Ge thickness, as shown in [20]. The optical response was measured up to an incident wavelength of 1650 nm with no clear cut-off. A significant drop in responsivity was observed, decreasing from 49 mA/W at 1530 nm to 39 mA/W at 1550 nm, and 3 mA/W at 1650 nm. The responsivity approximately decreases one decade per 100 nm increment in wavelength. This gradual decline can be attributed to the increase in absorption depth, but also to indirect absorption, strain in the buried Ge layers directly deposited on the Si substrate, and/or defect-related absorption, all of which broaden the absorption spectra [25]. Nevertheless, the PureGaB photodiode yielded a local responsivity maximum within the O-band for short-range communication, while being optically responsive in both telecom wavelengths of 1310 nm and 1550 nm.

In the DUT, the formation of acceptor states is expected where the Al has migrated through the semiconductors and doped them accordingly. The TEM images indicate that such p-doping could form at localized regions around the interface, being assisted by the presence of dislocations across the Ge-Si interface. Any p-doping or deep-level acceptor traps at the Ge-Si interface would result in a potential barrier for electron transport as illustrated in Fig. 3. To further assess the impact of the Ge-Si interface on device performance, the device was cooled down, and responsivity was measured at 250 K, 150 K, and 77 K. As seen in Figs. 2(b)–2(d), these measurements reveal deterioration of the optical response as the temperature decreases. The reduction is particularly strong for wavelengths above the cut-off wavelength of the Si (≈ 1100 nm), for which all the optical generation can be attributed to absorption in Ge. By cooling the device down to 77 K, the optical response above 1100 nm degrades more than an order of magnitude, leading to the conclusion that specifically the collection of carriers photogenerated in the Ge islands is suppressed by cooling. Notably, the low-temperature responsivity for wavelengths < 1100 nm degrades much less, though also being influenced by a reduced Ge response. This suggests that the collection of charge carriers photogenerated in Si has a much weaker temperature dependence than that of carriers in Ge. A qualitative explanation of this statement is provided in Fig. 3(a) and 3(b). When photons are absorbed in the Ge, as depicted in Fig. 3(a), photogenerated carriers are separated by the electric field. Due to the light doping of the Si (10^{15} cm^{-3}) compared to the Ge doping of about 10^{16} cm^{-3}, a small potential barrier in the conduction band is inherently present at the Ge-Si interface, having a value of about 0.1 eV. This barrier will have a negative effect on the collection of electrons generated in the Ge at the Si cathode. This situation could be ameliorated by processing a highly n-doped Si region, either in the form of an n$^+$-type Si bulk

Optics EXPRESS

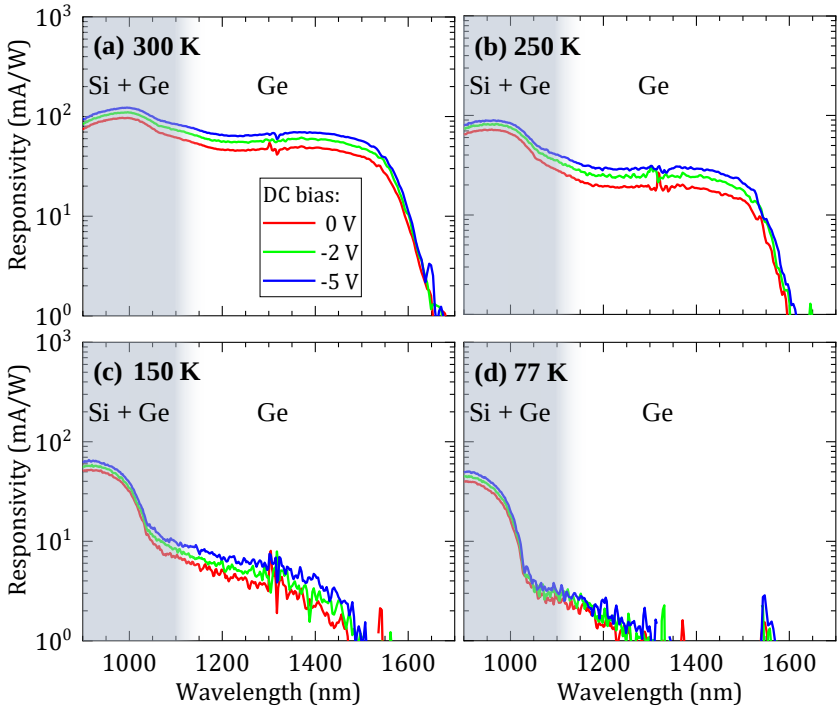

Fig. 2. Spectral responsivity of PureGaB Ge-on-Si photodiodes at four different temperatures: 300 K, 250 K, 150 K, and 77 K. The gray shading is used to discern between wavelengths absorbed by Si and Ge, or Ge only.

wafer or a locally arsenic or phosphorus n^+-implanted Si region. The latter would also be of interest for the isolation of photodiodes when using p-type substrates. There would, however, be a trade-off between capacitance and series resistance when considering operation speed. Figure 3 also indicates how this small potential barrier would be enhanced by the presence of acceptor states. The thermionic emission over this peaked Ge-Si barrier would be temperature-dependent. Photogenerated carriers blocked by the interfacial barrier remain undetected and eventually recombine, an effect which can be additionally enhanced by recombination at interfacial traps. However, if absorption occurs in Si, both types of generated carriers can reach their respective electrodes without being impeded by this interfacial barrier, as illustrated in Fig. 3(b).

Figure 2 also shows an increase in responsivity with increasing reverse bias. The effect is more pronounced for wavelengths above 1100 nm, indicating comparably higher bias dependence of collection efficiency in the Ge compared to the Si. This substantiates our previous conclusion: the increasing reverse bias depletes the p-doped interface, thus lowering the potential barrier for electrons, as shown in Fig. 3(c), and increasing the responsivity. Capacitance-voltage (*C-V*) measurements were performed to determine the depletion width at zero bias. An area-perimeter analysis was performed on diode samples with dimensions of $26 \times 26\,\mu m^2$, $24 \times 24\,\mu m^2$ and $12 \times 12\,\mu m^2$ to determine the area-dependent component of the diode capacitance. The area component was calculated to be 122 fF and 126 fF, corresponding to a depletion width of 795 nm and 770 nm for $26 \times 26\,\mu m^2$ diodes with 30-min and 60-min alloying times, respectively. These results indicate that the 500 nm-thick Ge layer was already fully depleted at zero bias. Therefore, further widening of the depletion region with bias continues into the Si, which does not contribute to the IR responsivity above 1100 nm or its contribution should be limited to small biases close to zero.

Optics EXPRESS

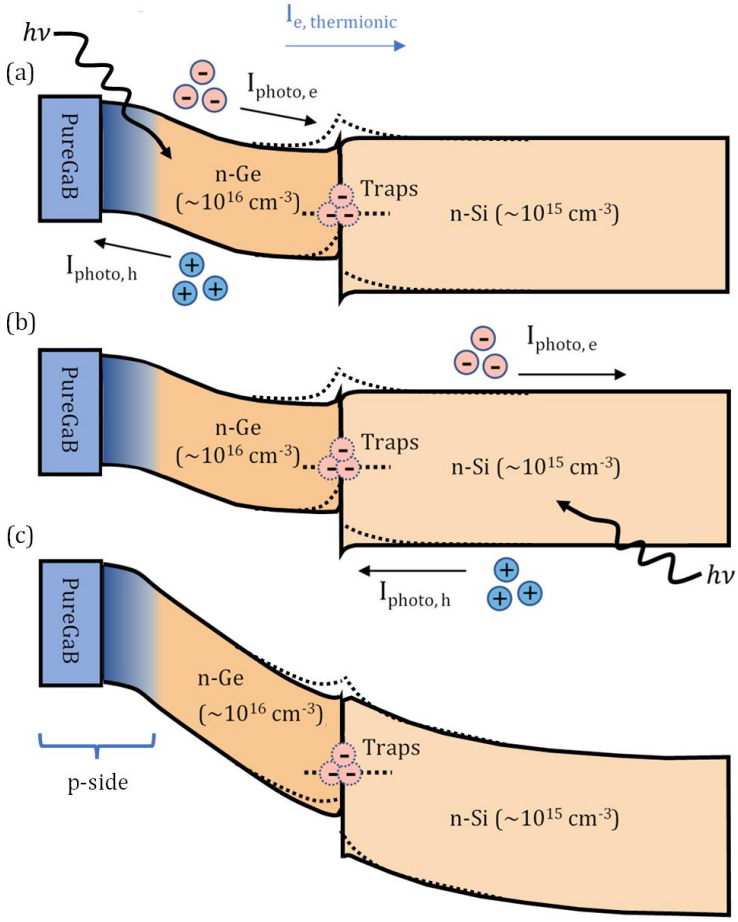

Fig. 3. Schematic of the energy band structure of PureGaB photodiodes. Separation of generated carriers at zero bias is shown for absorption in (a) Ge and (b) Si. A potential barrier (dashed) blocking the thermionic emission of electrons over the Ge-Si interface is related to acceptor states. (c) Band structure at high reverse bias.

To further investigate the lowering of the potential barrier with bias, focused monochromatic measurements at 1310 nm and 1550 nm were performed at RT. The optical measurements were performed on PureGaB photodiodes with both 30-min and longer 60-min alloying. As verified by more extensive alloying experiments in [17], the extra alloying reduces the ideal forward current, here by a factor of three, as shown in Fig. 4. This is presumably due to more p-doping of the Ge-Si interface region. Therefore, the reverse current near zero bias is also lower in the 60-min alloy case. However, the reverse current of these devices increases more steeply than for the 30-min-alloy devices, which is due to a lower breakdown voltage, 24 V as compared to 35 V for the 30-min-alloy devices. This difference is no doubt due to a small difference in the arsenic doping of the Ge, which is about $10^{16}\,\mathrm{cm}^{-3}$ but not entirely well-controlled. To avoid detrimental effects and noise in the responsivity measurements associated with avalanching/breakdown, the maximum bias voltage was limited to 18 V. The dark current of the 30-min-alloy devices shows a continuous increase from zero to 18 V reverse bias. This agrees well with the *C-V* results and indicates that the depletion region extends to the heterojunction even at zero bias. No carrier multiplication is observed in the reverse current up to 18 V reverse bias. The series resistance

Optics EXPRESS

extracted from the forward current was approximately 640 Ω for the 30-min-alloy and 570 Ω for the 60-min-alloy devices. Despite the relatively high series resistance of the 11-nm-thick PureB layer, which is not optimized for high-speed operation, the estimated RC bandwidth exceeds 2 GHz.

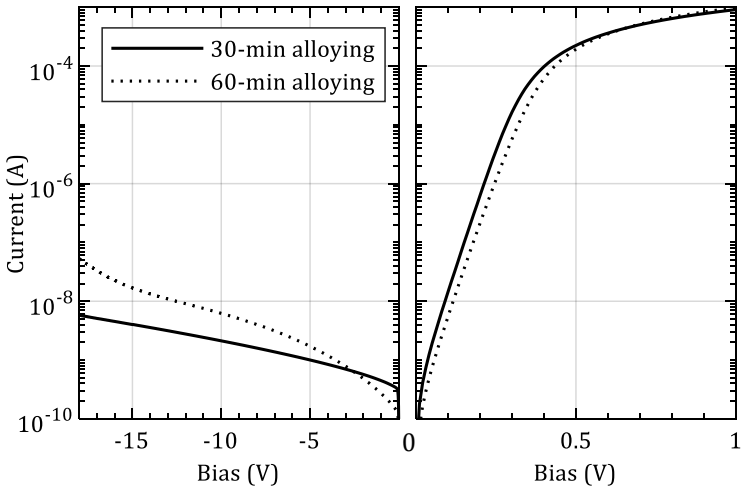

Fig. 4. Dark currents of PureGaB Ge-on-Si diodes with different alloying times of the Al used for contact metallization.

The photocurrent varies between samples due to the varying incident power but is at least a decade higher than the dark current, even at the highest biases. In all devices, the photocurrent also increases with the reverse bias, but faster than the dark current. To properly address the difference in the bias dependence between photo and dark current, the responsivity is calculated as $R = (I_{ph} - I_{dark}) / P_{DUT}$, where P_{DUT} is the incident optical power focused to DUT. The responsivity of PureGaB diodes exhibited a continuous and monotonic increase up to 18 V, as depicted in Fig. 5(a).

As the Ge region is fully depleted, the persistent rise in responsivity with increasing bias is attributed to the lowering of the Ge-Si interfacial barrier. Up to 18 V, the average responsivity increased ~2.3 times compared to the unbiased diodes at both 1310 nm and 1550 nm, asymptotically approaching the value expected when there is no interfacial barrier in the conduction band. These findings were consistent across various diodes on the same die. Furthermore, RT measurements were repeated on devices with the longer Al-alloying time, which should enhance Al-mediated material transport.

The responsivity of PureGaB photodiodes with prolonged alloying is shown in Fig. 5(b). With the prolonged Al-alloying, average responsivity at zero bias deteriorated by a factor of ~15 at both 1310 nm and 1550 nm. This indicates that the 5-μm-wide ring displaying a clear displacement of materials in the 30-min-alloy devices, probably now covers the whole diode interface area. Therefore, in the 60-min-alloy devices, the barrier behavior is surely due to material transport, and not only the inherent potential barrier and interface defects that possibly are the sole cause of barrier behavior in the center of the 30-min-alloy devices. However, increasing the bias reduces the Ge-Si potential barrier in the case of both devices. Still, the 60-min-alloy devices exhibit a sharper, exponential increase in responsivity up to 8 V reverse bias. After that, the increase slows down approaching the responsivity figure of the 30-min-alloy devices. From zero to 18 V reverse bias, the average responsivity of these diodes increased 34 and 43 times at 1310 nm and 1550 nm, respectively. Above 15 V reverse voltage responsivity at 1310 nm is about equal in both device sets. However, at 1550 nm, in 60-min-alloy devices, responsivity is notably higher

Optics EXPRESS

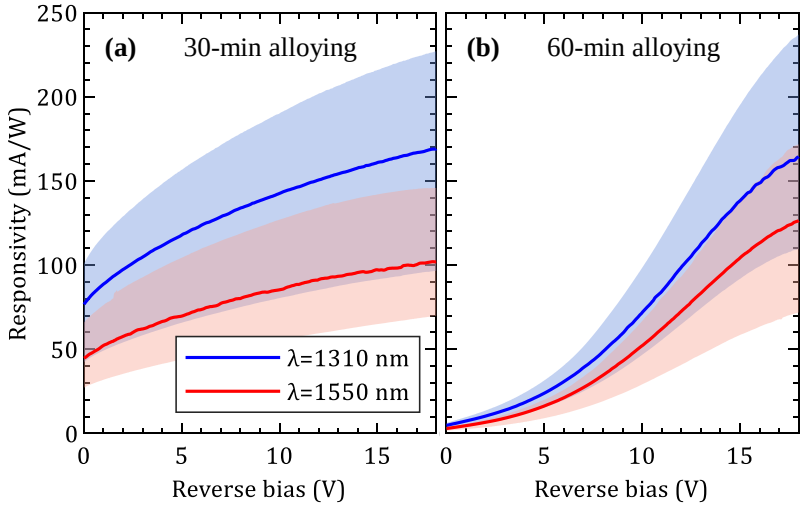

Fig. 5. Bias-dependent responsivity of PureGaB Ge-on-Si diodes (a) upon standard 30-min alloying of Al used for contact metallization and (b) diodes with alloying prolonged to 60 minutes. Solid lines represent the average responsivity. The shaded area represents the range between minimum and maximum responsivity.

compared to the 30-min-alloy samples. Prolonged alloying caused the responsivity to increase at 1550 nm and 18 V, from 102.0 mA/W to 126.4 mA/W. This effect may be attributed to the passivation of the Ge-Si interface, similar to what occurs with the diode sidewalls, improving the absorption of wavelengths deep within the Ge and near the interface. This demonstrates that the negative effects of the Ge-Si interface barrier on responsivity can be mitigated by increasing the standard operating reverse bias in fully depleted Ge-on-Si devices fabricated on lightly doped Si substrates.

4. Conclusion

Through temperature- and voltage-dependent responsivity measurements, the impact of potential barriers at the Ge-Si interface of Ge-on-Si photodiodes was investigated in the NIR spectral range. For photogenerated carriers in the Ge, an inherent potential barrier for electron collection at the Si cathode exists at the Ge-Si interface due to the bandgap difference as well as any acceptor-type interface traps. Such a barrier was shown to be aggravated by the Al passivation of the Ge sidewalls and associated Al-Ge-Si material migration along the Ge-Si interface. By creating Al-doped acceptor states, this migration process was beneficial for reducing the dark current, but at low voltages, the RT responsivity at IR wavelengths was seriously degraded and practically extinguished at cryogenic temperatures down to 77 K. However, in the present devices, the RT responsivity was increased manifold by applying reverse voltages up to 18 V to pull down the interface barrier. In the devices that suffered from the highest barriers, the responsivity at 1310 nm increased from 4.8 to 164 mA/W, at 0 V and 18 V, respectively. Thus, the responsivity took on values close to those ideally expected for Ge islands with a thickness of 0.5 µm. In addition, if the Al-migration process reaches the interface, it provides a relative improvement in responsivity near the long-wavelength absorption edge compared to shorter wavelengths. If the detector design allows such high-voltage biasing of the Ge photodiode, there could be new potentials for on-chip integration of low-dark current, high-responsivity Ge-on-Si photodiodes as demonstrated in this work. The need to have a highly n-doped Ge-Si interface is reduced, and the use of Al-sidewall passivation of the Ge islands to lower dark currents and enhance long-wavelength response becomes a viable option.

Optics EXPRESS

Funding. Croatian Science Foundation (IP-2022-10-5294); NextGenerationEU (NPOO.C3.2.R2-I1.06.0025); HORIZON-RIA (101070441).

Acknowledgments. This work was performed, in part, at the Integrated NanoMaterials Laboratory (INML) at the California NanoSystems Institute (CNSI), University of California Los Angeles (UCLA).

Disclosures. The authors declare no conflicts of interest.

Data availability. Data underlying the results presented in this paper are not publicly available at this time but may be obtained from the authors upon reasonable request.

References

1. J. Michel, J. Liu, and L. C. Kimerling, "High-performance Ge-on-Si photodetectors," Nat. Photonics **4**(8), 527–534 (2010).
2. J. Cui and Z. Zhou, "High-performance Ge-on-Si photodetector with optimized DBR location," Opt. Lett. **42**(24), 5141 (2017).
3. L. Virot, P. Crozat, J.-M. Fédéli, *et al.*, "Germanium avalanche receiver for low power interconnects," Nat. Commun. **5**(1), 4957 (2014).
4. P. Vines, K. Kuzmenko, J. Kirdoda, *et al.*, "High performance planar germanium-on-silicon single-photon avalanche diode detectors," Nat. Commun. **10**(1), 1086 (2019).
5. M. A. Khalighi and M. Uysal, "Survey on Free Space Optical Communication: A Communication Theory Perspective," IEEE Commun. Surv. Tutorials **16**(4), 2231–2258 (2014).
6. C.-P. Hsu, B. Li, B. Solano-Rivas, *et al.*, "A Review and Perspective on Optical Phased Array for Automotive LiDAR," IEEE J. Select. Topics Quantum Electron. **27**(1), 1–16 (2021).
7. U. Younis, S. K. Vanga, A.E. J. Lim, *et al.*, "Germanium-on-SOI waveguides for mid-infrared wavelengths," Opt. Express **24**(11), 11987–11993 (2016).
8. L. M. Giovane, H.-C. Luan, A. M. Agarwal, *et al.*, "Correlation between leakage current density and threading dislocation density in SiGe pin diodes grown on relaxed graded buffer layers," Appl. Phys. Lett. **78**(4), 541–543 (2001).
9. A. Sammak, W. De Boer, and L. K. Nanver, "Ge-on-Si: Single-crystal selective epitaxial growth in a CVD reactor," ECS Trans. **50**(9), 507–512 (2013).
10. L. Marković, T. Knežević, L. K. Nanver, *et al.*, "Modeling and Simulation Study of Electrical Properties of Ge-on-Si Diodes with Nanometer-thin PureGaB Layer," in *44th International Convention on Information, Communication and Electronic Technology* (IEEE, 2021), pp. 64–69.
11. L. Shi, S. Nihtianov, L. Haspeslagh, *et al.*, "Surface-charge-collection-enhanced high-sensitivity high-stability silicon photodiodes for DUV and VUV spectral ranges," IEEE Trans. Electron Devices **59**(11), 2888–2894 (2012).
12. A. Sammak, M. Aminian, L. Qi, *et al.*, "(Invited) Fabrication of Pure-GaB Ge-on-Si Photodiodes for Well-Controlled 100-pA-Level Dark Currents," ECS Trans. **64**(6), 737–745 (2014).
13. L.K. Nanver, T. Knezevic, X. Liu, *et al.*, "On the Many Applications of Nanometer-Thin Pure Boron Layers in IC and Microelectromechanical Systems Technology," J. Nanosci. Nanotechnol. **21**(4), 2472–2482 (2021).
14. T. Knežević, M. Krakers, and L. K. Nanver, "Broadband PureGaB Ge-on-Si photodiodes responsive in the ultraviolet to near-infrared range," in *Optical Components and Materials XVII 11276* (SPIE, 2020), pp. 73–85.
15. M. Krakers, T. Knežević, and L. K. Nanver, "Optoelectrical Operation Stability of Broadband PureGaB Ge-on-Si Photodiodes with Anomalous Al-Mediated Sidewall Contacting," J. Electron. Mater. **50**(12), 7026–7036 (2021).
16. A. Sammak, L. Qi, and L. Nanver, "Restricted-access Al-mediated material transport in Al contacting of PureGaB Ge-on-Si p+ n diodes," J. Electron. Mater. **44**(12), 4676–4683 (2015).
17. A. Sammak, M. Aminian, L.K. Nanver, *et al.*, "CMOS-compatible PureGaB Ge-on-Si APD pixel arrays," IEEE Trans. Electron Devices **63**(1), 92–99 (2016).
18. D. T. Shivakumar, T. Knežević, and L. K. Nanver, "Nanometer-thin pure boron CVD layers as material barrier to Au or Cu metallization of Si," J. Mater. Sci.: Mater. Electron. **32**(6), 7123–7135 (2021).
19. P. Tsipas and A. Dimoulas, "Modeling of negatively charged states at the Ge surface and interfaces," Appl. Phys. Lett. **94**(1), 012114 (2009).
20. L. K. Nanver, V. V. Hassan, A. Attariabad, *et al.*, "Broadband PureB Ge-on-Si photodiodes," IEEE Electron Device Lett. **45**(6), 1040–1043 (2024).
21. T. Nishida, M. Nakata, T. Suemasu, *et al.*, "Minority carrier lifetime of Ge film epitaxial grown on a large-grain seed layer on glass," Thin Solid Films **681**, 98–102 (2019).
22. Z.M. Wang, J.Y. Wang, L.P.H. Jeurgens, *et al.*, "Investigation of metal-induced crystallization in amorphous Ge/crystalline Al bilayers by Auger microanalysis and selected-area depth profiling," Surf. Interface Anal. **40**(3-4), 427–432 (2008).
23. Y. Zhang, X. Shao, Y. Zhang, *et al.*, "Correction of FTIR acquired photodetector response spectra from mid-infrared to visible bands using onsite measured instrument function," Infrared Phys. Technol. **92**, 78–83 (2018).
24. L. Vivien, M. Rouvière, J.-M. Fédéli, *et al.*, "Ge photodetectors integrated in Si waveguides," in *Silicon Photonics III. 6898* (SPIE, 2008), p. 689815.
25. K. Noguchi, M. Nishimura, Y. Tsusaka, *et al.*, "Enhancement of L-band optical absorption in strained epitaxial Ge on Si-on-quartz wafer: Toward extended Ge photodetectors," J. Appl. Phys. **128**(13), 133107 (2020).